Available online at www.sciencedirect.com
ScienceDirect
Journal of Nuclear Materials 373 (2008) 157–163
journal of nuclear materials
www.elsevier.com/locate/jnucmat

Production and reaction kinetics of radiation-induced defects in α-alumina and sapphire under ion beam irradiation

Kimikazu Moritani, Yoichi Teraoka, Ikuji Takagi, Masafumi Akiyoshi, Hirotake Moriyama *

Department of Nuclear Engineering, Graduate School of Engineering, Kyoto University, Yoshida, Sakyo-ku, Kyoto 606-8501, Japan

Received 30 September 2006; accepted 1 June 2007

Abstract

The production behavior of radiation-induced defects in α-alumina and sapphire was studied by in situ luminescence measurement technique under ion beam irradiation of He^+. The irradiation time dependence of the luminescence intensities of the F^+ centers and F^0 centers at 330 nm and 420 nm, respectively, was measured at each temperature from 298 to 523 K. By considering that the luminescence intensities represent the accumulated F^+ and F^0 centers, the observed irradiation time dependence was analyzed to obtain the rate constants for the production and reaction kinetics of radiation-induced defects of F-type centers.

PACS: 61.80.Jh; 61.72.Cc

1. Introduction

Irradiation behavior of ceramic materials has been studied for many years [1]. However, the dynamic production behavior of radiation-induced defects under irradiation has not been fully clarified in spite of the considerable progress in understanding many aspects of radiation-induced defects in these ceramic materials. It is thus important to know the production behavior of radiation-induced defects by such an in situ luminescence measurement technique, which may be applied to monitor radiation-induced defects as reported previously [2].

In our previous study [2], the production behavior of radiation-induced defects in α-alumina and sapphire was studied by in situ luminescence measurement technique under ion beam irradiation of H^+ and He^+. An irradiation history was observed repeatedly with annealed specimens, in which the luminescence intensities increased with irradiation time and reached the steady state ones, and the possibility of using this technique to monitor radiation-induced defects was indicated. The steady state luminescence intensity of the F^+ centers at 330 nm was observed to decrease monotonically with the increasing temperature up to 800 K, while the intensity of the F^0 centers at 410 nm to show non-monotonic temperature-dependence. In the latter case, the intensity decreased with the temperature up to 600 K, and then increased above this temperature. These observations were successfully analyzed by considering the production mechanisms and reaction kinetics of the radiation-induced defects of F-type centers. In spite of successful analysis, however, it is still needed to improve our knowledge on the reaction kinetics since the first-order reactions have been assumed for all the reactions for simplicity.

Following our previous study [2], the irradiation time dependence of the luminescence intensities of the F^+ and F^0 centers was more extensively measured in the temperature range from 298 to 523 K in the present study. The measurement was made at the lower temperatures to decrease such effects as of thermal quenching. By considering that the luminescence intensities represent the accumulated F^+ and F^0 centers and by considering the second-order reactions, the observed irradiation time dependence was analyzed to

* Corresponding author. Tel./fax: +81 75 753 5824.
E-mail address: moriyama@nucleng.kyoto-u.ac.jp (H. Moriyama).

0022-3115/$ - see front matter © 2007 Elsevier B.V. All rights reserved.
doi:10.1016/j.jnucmat.2007.06.001

obtain the reaction rate constants for radiation-induced defects of F-type centers together with those for oxygen interstitials.

2. Experimental

Procedures were mostly the same as those in the previous study [2]. The pellet-type specimens of α-alumina (Al_2O_3: 99.9%, SiO_2: 0.04%, Na_2O: 0.02%, MgO: 0.01%, CaO: 0.01%, Fe_2O_3: <0.01% [3]) and sapphire were obtained from Kyocera Co. Ltd., which were of 10 mm in diameter and about 0.5 mm in thickness. Each specimen was irradiated with a He^+ ion beam, accelerated to 2 MeV with a Van de Graaff accelerator. The range and total number of displacements were estimated to be about 4 μm and 170 displacements/ion, respectively, by using the TRIM code (SRIM-98) with the displacement energies of 20 eV for Al and 50 eV for O. The size of the ion beam was about 2 mm × 2 mm and its current was monitored. A photonic multichannel analyzer, Hamamatsu PMA-11 was used to measure the irradiation time dependence of the luminescence. The temperature of the sample holder was controlled with an electric heater and a thermocouple while another thermocouple was attached to the sample surface to monitor its temperature at a distance close to beam area. In the room temperature irradiation, the temperature rise by beam heating was observed to be within a few degrees as estimated by taking the values of thermal diffusion coefficient, density and heat capacity of alumina. The experimental conditions are summarized in Table 1.

3. Results and discussion

3.1. Irradiation time dependence

The observed luminescence spectra are composed of a number of luminescence bands, namely 330 nm, 420 nm and others, as already reported [2], of which the luminescence bands centered at 330 and 420 nm can be attributed to the F^+ and F^0 centers, respectively [4].

Figs. 1 and 2 show typical results of the measurement of α-alumina and sapphire, respectively, in which the luminescence intensity is given in cps for a fixed window of 0.75 nm. It is shown that the luminescence intensities at 330 and 420 nm show an irradiation history in which the intensities increase with irradiation time and reach the maximum ones, and that the intensities decrease at the longer irradiation in some cases. By annealing the irradiated specimens above 1073 K for some 10 min, such an irradiation history has been observed repeatedly [2]. This fact suggests that a considerable part of the luminescence comes from the defects accumulated by irradiation and that the intensities at these bands may reflect the amounts of the F^+ and F^0 centers. A similar irradiation history for the ion beam induced luminescence of sapphire has been reported by Al Ghamdi and Townsend [5], who have observed non-zero values for the luminescence intensity at a low fluence and have suggested that the luminescence is from intrinsic color centers activated by excited electrons. In the present case, on the other hand, nearly zero values have been observed with annealed specimens, suggesting that the luminescence originates from the F^+ and F^0 centers accumulated by irradiation.

In the case of electron irradiated sapphire [6], it has been found that the peak height ratio between the F^+ and F^0 is strongly dependent on the dose rate and that the F^+ luminescence increases with the dose rate while the F^0 luminescence decreases. Since the F^+ is hardly accumulated in the electron irradiated sapphire, this dose rate effect has been explained by considering the conversion of the F^0 to the F^+; the F^0 is excited by electron and hole capture and this excited F^0 is ionized by hole capture giving the F^+ [6]. As already reported [2], on contrast, such a dose rate effect was hardly observed in the studied region, possibly due

Table 1
Experimental conditions and steady state luminescence intensity

Specimen	Irradiation condition			Steady state luminescence intensity (cps) at	
	Projectile	Temperature[a] (K)	Beam current (nA/cm^2)	330 nm	420 nm
α-Alumina	2 MeV He^+	298	63	⩾6000	≈2000
		298	81	⩾6000	≈1000
		423	164	⩾14000	≈2800
		423	238	≈8000	≈2000
		448	67	≈3500	≈600
		473	81	>4000	≈100
		473	131	≈13000	≈200
		523	77	≈4500	≈200
Sapphire	2 MeV He^+	298	66	≈8000	≈2800
		300	133	⩾6000	≈1700
		323	119	≈11000	≈2000
		373	514	≈25000	≈6000
		423	133	≈17000	≈6000
		448	75	⩾1400	≈500
		523	140	≈7000	≈300

[a] Temperature of the thermocouple attached to the sample surface to monitor its temperature.

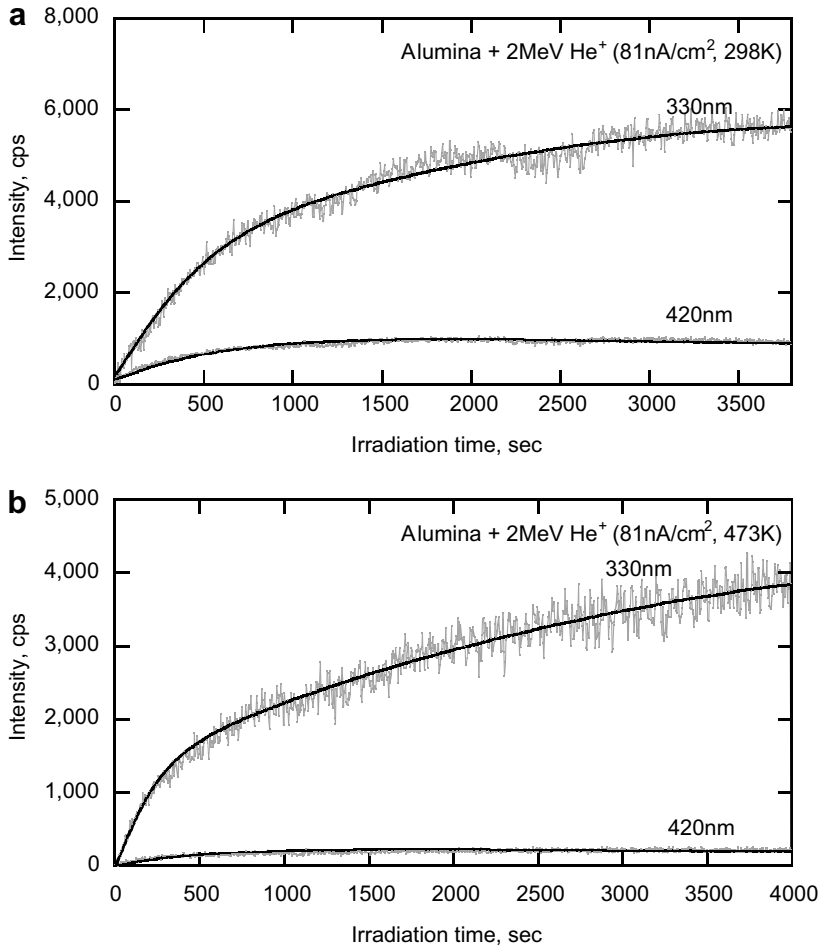

Fig. 1. Irradiation time dependence of the luminescence from α-alumina under 2 MeV He^+ irradiation at (a) 298 K and (b) 473 K. The luminescence intensity is given in cps for a fixed window of 0.75 nm. The specimen was annealed above 1073 K for 10 min.

to low dose rates compared with the above case. Thus the presently observed luminescence intensities at 330 and 420 nm are considered to represent the accumulated F^+ and F^0 centers, respectively.

3.2. Production and reaction mechanism of radiation-induced defects

In the case of ionic compounds such as alumina, it is considered that the formation of such F-type defect centers of the F^+ and F^0 is accompanied with the formation of the interstitial O^- and O^0, respectively. In addition to these, the O_2^- and O_2 may be formed by the reactions of $O^- + O^0 \rightarrow O_2^-$ and $O^0 + O^0 \rightarrow O_2$, although the diffusion of the O_2^- and O_2 will be much slower than the O^- and O^0. Also, the formation of some cluster defects, denoted by F_x inclusively, may be expected from the reactions of F-type defect centers. Thus, similarly to the previous study [2], but considering only the reactions at relatively lower temperatures of the present study, the following production and reaction mechanism of radiation-induced defects in α-alumina and sapphire can be suggested:

$$Al_2O_3 \rightarrow Al_2O_3^* \rightarrow F^+ + O^-, \quad (0a)$$

$$Al_2O_3 \rightarrow Al_2O_3^* \rightarrow F^0 + O^0, \quad (0b)$$

$$F^+ + O^- \rightarrow \text{recombination}, \quad (1a)$$

$$F^0 + O^0 \rightarrow \text{recombination}, \quad (1b)$$

$$O^- + O^0 \rightarrow O_2^-, \quad (2a)$$

$$O^0 + O^0 \rightarrow O_2, \quad (2b)$$

$$F^+ + F_x \rightarrow F_x, \quad (3)$$

$$F^0 + F^0 \rightarrow F_x, \quad (4a)$$

$$F^0 + F_x \rightarrow F_x. \quad (4b)$$

Reactions (0a) and (0b) represent the production of the F^+ and F^0, respectively, through an excited Al_2O_3 ($Al_2O_3^*$) by ion beam irradiation. Reactions (1a) and (1b) represent the recombination of the F^+ and F^0 with the O^- and O^0, respectively, while reactions (2a) and (2b) the formation of the O_2^- and O_2. Because of their larger sizes, the O_2^- and O_2 are considered to be hardly responsible for further reactions at the lower temperatures. Reactions 3, 4a and 4b represent the formation of cluster defects F_x. It is important to note that the reaction rate constants are treated

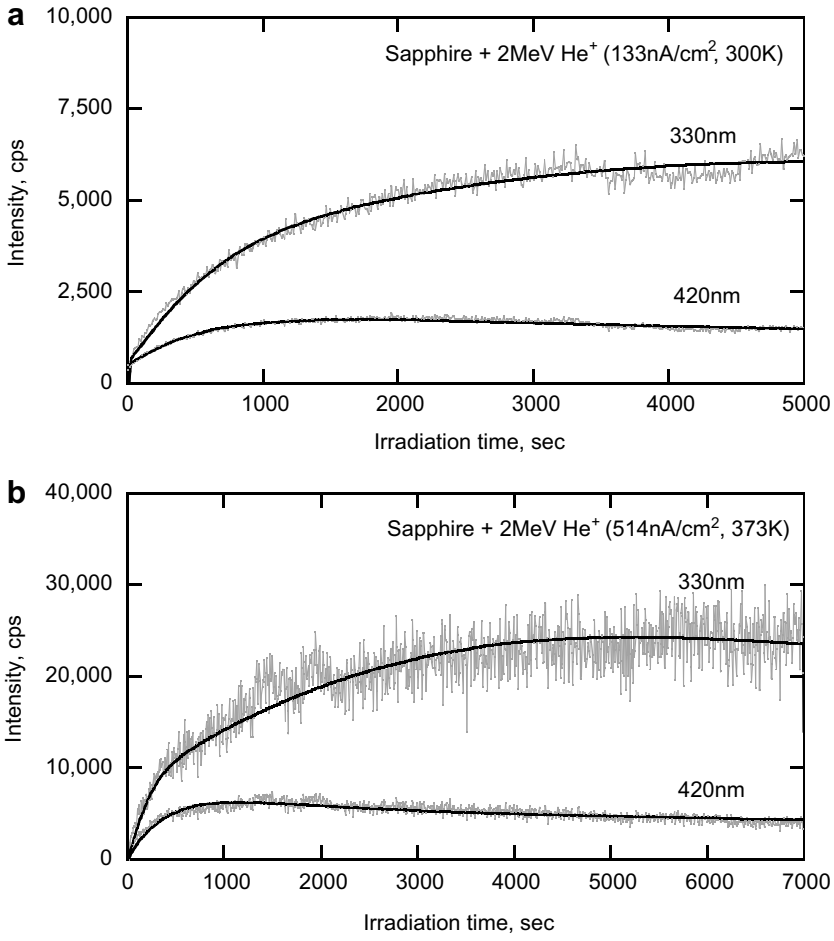

Fig. 2. Irradiation time dependence of the luminescence from sapphire under 2 MeV He^+ irradiation at (a) 300 K and (b) 373 K. The luminescence intensity is given in cps for a fixed window of 0.75 nm. The specimen was annealed above 1073 K for 10 min.

as the same for similar reactions in the following analysis for simplicity; k_1 for reactions 1a, 1b, 2a and 2b, k_3 for reaction (3), and k_4 for reactions (4a) and (4b). The values of the rate constants may be given in atomic fraction for example.

3.3. Determination of reaction rate constants

It is interesting and important to obtain the rate constants of reactions involved in the production of radiation-induced defects. Once the rate constants are obtained, one can predict the accumulation behavior of the radiation-induced defects at various conditions. Based on the suggested reaction scheme, the observed irradiation time dependence of the luminescence intensity is analyzed here to obtain such rate constants.

According to the literature [4], the luminescence at 3.8 eV (325 nm) is attributed to the singlet (2P to $1S^*$) emissions of the F^+ centers and 3.0 eV (410 nm) the triplet (^3P to $^3S^*$) of the F^0 centers. Considering that the luminescence is caused from the F^+ and F^0 activated by excited electrons or electron–hole pairs, the observed luminescence intensities I_{330} and I_{420} at 330 nm and 420 nm are proportional to the state densities of $[F^+(1A)]$ and $[F^0(^1S)]$, as given by:

$$I_{330} = \varepsilon_{F+}\phi[F^+(1A)], \tag{5}$$

$$I_{420} = \varepsilon_{F0}\phi[F^0(^1S)], \tag{6}$$

where ε_{F+} and ε_{F0} represent the luminescence detection efficiencies including geometric factors and excitation probabilities and ϕ the ion beam current. The variation of the state densities of $[F^+(1A)]$ and $[F^0(^1S)]$ with irradiation time can be calculated by solving the following equations:

$$d[F^+]/dt = g_{F+}\phi - k_1[F^+][O^-] - k_3[F^+][F_x], \tag{7}$$

$$d[F^0]/dt = g_{F0}\phi - k_1[F^0][O^0] - 2k_4[F^0]^2 - k_4[F^0][F_x], \tag{8}$$

$$d[O^-]/dt = g_{F+}\phi - k_1[F^+][O^-] - k_1[O^-][O^0], \tag{9}$$

$$d[O^0]/dt = g_{F0}\phi - k_1[F^0][O^0] - k_1[O^-][O^0] - 2k_1[O^0]^2, \tag{10}$$

$$d[F_x]/dt = k_4[F^0]^2, \tag{11}$$

where g_{F+} and g_{F0} are the generation rate of F^+ and F^0 by reactions (0a) and (0b), respectively. One can estimate the values of the g_{F+} and g_{F0} from a conversion factor of 1 dpa (for oxygen) $= 1.08 \times 10^{17}$ ions/cm^2 (2.0 eV He^+), which is obtained as a weighted average value along ion

tracks by using the TRIM code (SRIM-98) with the displacement energies of 20 eV for Al and 50 eV for O. Considering the fractions of the surviving defects from cascade reactions, one tenth of the conversion factor is temporarily taken for each of the g_{F+} and g_{F0} in the present study.

For the analysis of the observed results, Eqs. (7)–(11) are solved by the Runge–Kutta method to obtain the steady state densities of the F^+ and F^0 which are substituted into Eqs. (5) and (6). As already mentioned above, the reaction rate constants are treated as the same for similar reactions in the present analysis; k_1 for reactions 1a, 1b, 2a and 2b, k_3 for reaction (3), and k_4 for reactions (4a) and (4b). The measured luminescence intensity data were fitted to Eqs. (5) and (6) combined with Eqs. (7)–(11) by the least-squares method, and the parameter values were obtained. As shown in Figs. 1 and 2, the agreements are satisfactorily good in all the cases.

As typical results of the present analysis, Fig. 3(a) and (b) show the variations of the defect densities with irradiation time in alumina and sapphire, respectively, which are simulated by using the obtained parameter values for the observed luminescence in Figs. 1(a) and 2(b). The densities of the O^- and O^0 reach the steady state rapidly, and those of the F^+ and F^0 follow to reach little slowly. Different kinetics of the F^+ and F^0 are shown in the figure, in which the density of the F^+ increases rather monotonically while the F^0 increases and then decreases. This difference may be due to different rate constants in Eqs. (7) and (8); the k_3 for reaction (3) will be smaller than the k_4 for reactions (4a) and (4b) possibly because of some repulsive forces between the F^+ and positively charged F_x. It is interesting to point out that the formation of the cluster defects F_x starts above the dpa value of 10^{-3}, for comparison with the results of other methods such as optical absorption measurements [1].

Fig. 4(a), (b) and (c) show the Arrhenius plots of the rate constants of k_1, k_3 and k_4, respectively, which are obtained from the present analysis. No apparent difference is observed for α-alumina and sapphire. As shown in Table 2, the Arrhenius equations of the rate constants

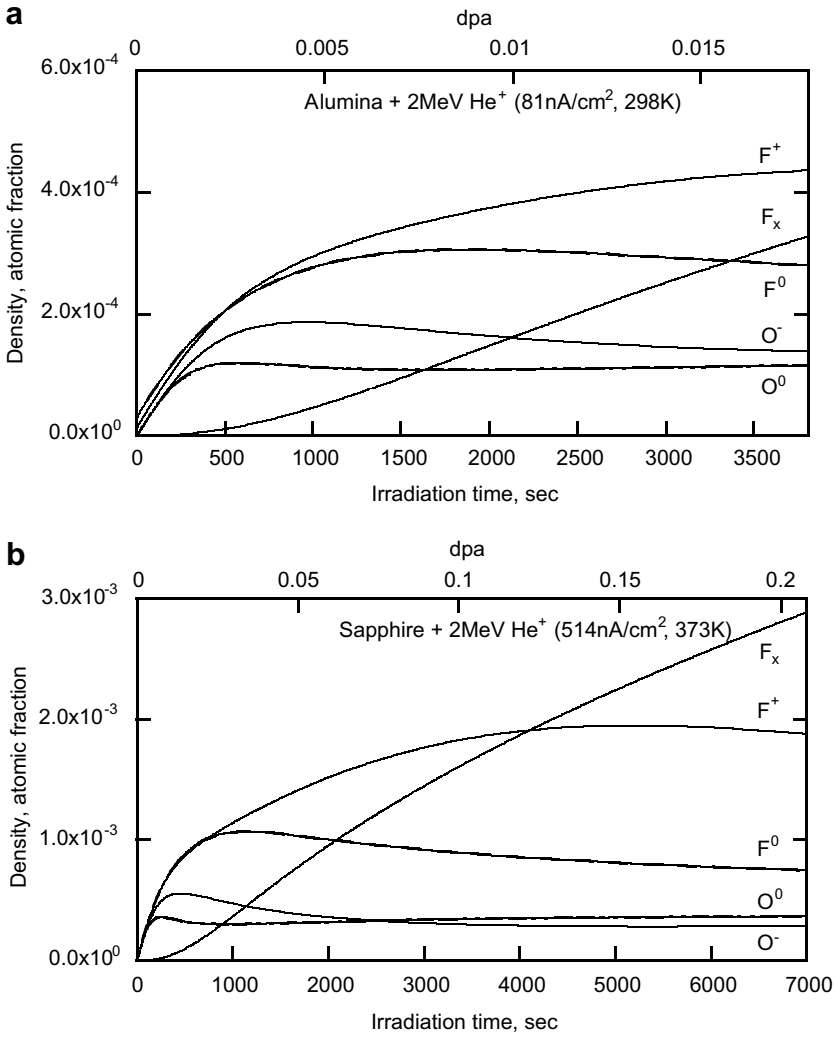

Fig. 3. Accumulation behavior of radiation-induced defects in (a) α-alumina and (b) sapphire under 2 MeV He^+ irradiation. Curves represent the results of simulation for the observed luminescence in Figs. 1(a) and 2(b).

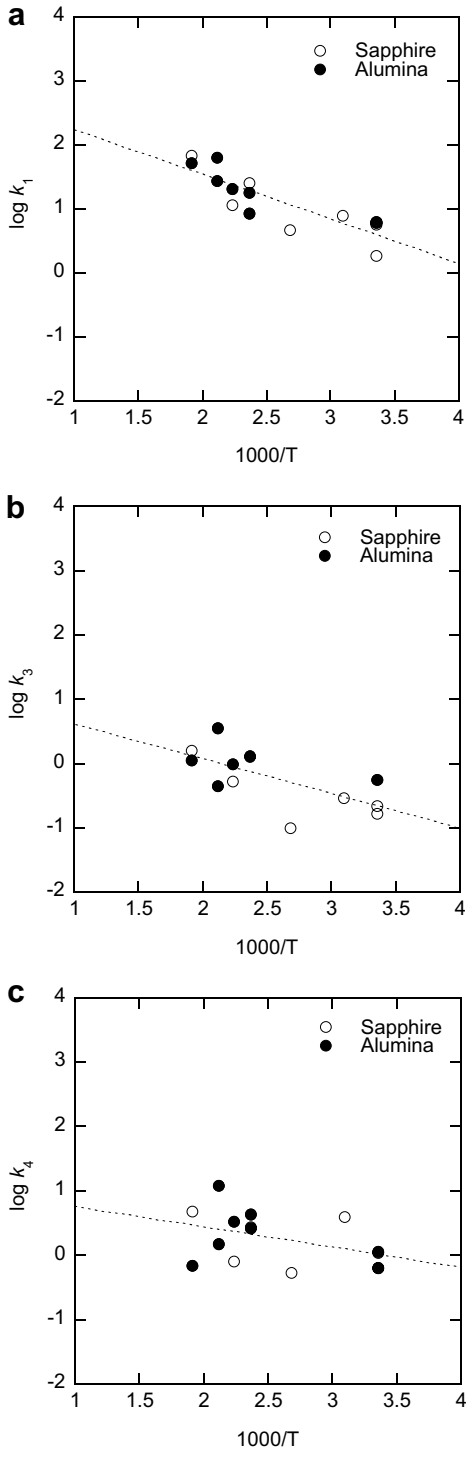

Fig. 4. Arrhenius plots of rate constant of (a) k_1, (b) k_3 and (c) k_4. Curves represent the least-squares fitting of the data to Arrhenius equation in Table 2.

are obtained by the least-squares fitting, and the activation energies are obtained to be 0.14 ± 0.03, 0.11 ± 0.03, and 0.07 ± 0.04 eV for k_1, k_3 and k_4, respectively. According to a comprehensive review of Zinkle and Kinoshita [1], there is relatively little information available on the interstitial migration energies for Al_2O_3, though it appears that both Al and O interstitials are mobile in Al_2O_3 near and below room temperature. It can be considered that reactions 1a,1b,2a,2b may be limited by the migration of O, of which the activation energy is obtained to be 0.14 eV in the present study. As for the k_3 and k_4, it is noticed that the activation energies of 0.11 and 0.07 eV are considerably small compared with the migration energies of 1.8–2 eV [1] for O vacancies. An explanation for this difference is as follows. In the case of ion irradiation, there will be overlaps of ion tracks, which increase with the increasing dpa value. Then, defects once formed, including not only point defects of the F^+ and F^0 but also cluster defects F_x, may be involved in another ion track in which reactions (3) to (4b) proceed. The activation energies of such reactions will be small as observed in the present study.

Table 2
Reaction rate constants obtained from the analysis of in situ luminescence measurement data

Rate constants	$k_i = A_i \exp[-E_i/kT]$	
	A_i	E_i (eV)
k_1	$10^{2.9\pm0.3}$	0.14 ± 0.02
k_3	$10^{1.2\pm0.5}$	0.11 ± 0.03
k_4	$10^{1.1\pm0.5}$	0.06 ± 0.04

It is interesting to compare the present results with the literature ones. One is for oxygen interstitials. In the case of alkali halides, different types of oxygen interstitial traps, extrinsic and intrinsic, are known to be present and to affect the F-coloring and F-thermal-annealing curves [7]. Similarly to the case of alkali halides, it has been reported that there are different components related to the different types of oxygen interstitial traps in sapphire under electron beam irradiation [8]. In that case, two types of interstitial traps were identified, of which the activation energies for detrapping the interstitial were obtained to be 0.32 and 0.18 eV. Compared with those results, a little lower value of 0.14 eV is obtained in the present study, not for the detrapping but for the migration of interstitials. Under the present conditions of ion beam irradiation, an efficient defect production occurs and results in a relatively higher concentration of interstitials. The effects of various interstitial traps other than the F-type centers are thus negligible, similarly to the case of alkali halides exposed to high dose [9], and the activation energy for the migration of interstitials is successfully determined in the present case.

Another one is for the cluster defects F_x. Considering the F_x curve in Fig. 3, one would expect the observation of the F_x in the present specimens. In fact, such aggregate centers as F_2^+ and F_2 have been identified to be formed in neutron-irradiated single crystal α-Al_2O_3 [10]. For comparison, some specimens of sapphire in the present study were subjected to the absorption measurement, but only a slight and broad absorption was observed over the range studied from 200 to 800 nm. This might be due to too small (narrow and thin) damage regions which are confined within

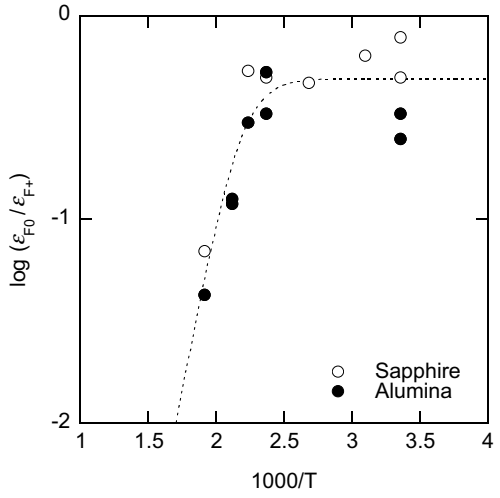

Fig. 5. Arrhenius plots of the ratio of the luminescence detection efficiency of the F^0 to that of the F^+. Curve represents the least-squares fitting of the data to Eq. (12).

less than 1% of the specimen volume in the present case. Also, no apparent luminescence of such aggregate centers was identified in the observed luminescence spectra, as reported in our previous study [2]. Considering possible formation of Al colloids at higher doses, more careful measurements may be needed for observation and details of the F_x.

As for the luminescence detection efficiency, different temperature dependences of the ε_{F+} and ε_{F0} were obtained in the analysis; the ε_{F+} is almost constant while the ε_{F0} decreases at the higher temperatures above 450 K. Then, by eliminating the scatters due to the geometric factors, the ratio of the luminescence detection efficiency of the F^0 to that of the F^+ is plotted in Fig. 5. It can be seen that the $\varepsilon_{F0}/\varepsilon_{F+}$ rapidly decreases like a thermal quenching. The following equation is thus tentatively applied for the analysis, which has originally been applied to temperature-dependent F center luminescence in alkali halides by Swank and Brown [11]

$$(\varepsilon_{F0}/\varepsilon_{F+}) = C/[1 + (\tau_R/\tau_0)e^{-\Delta E/kT}], \quad (12)$$

where C is a constant, τ_R a radiative life time, and $(1/\tau_0)e^{-\Delta E/kT}$ the probability of thermal activation into a nonradioactive decay channel, with activation energy ΔE. In the present case, the parameter values are obtained to be $C = 10^{-0.31 \pm 0.07}$, $(\tau_R/\tau_0) = 10^{7.80 \pm 1.72}$ and $\Delta E = 0.70 \pm 0.17$ eV. For details of this thermal quenching, it is noticed that, in addition to thermal ionization, there may be possible contributions of such an ionization of the F^0 by hole capture at some conditions, as suggested for electron irradiated sapphire [6]. Further studies are thus needed for the reaction kinetics above 450 K.

4. Conclusions

The observed irradiation time dependence of the luminescence intensity under irradiation was confirmed to reflect the accumulation behavior of radiation-induced defects by its reproducibility with annealing. The results were successfully analyzed by considering a production and reaction mechanism of radiation-induced defects, which included the formation of cluster defects. By taking an estimated generation rate for point defects, the accumulation behavior of radiation-induced defects was obtained in the unit of atomic fraction. It was shown that the formation of the cluster defects F_x starts above the dpa value of 10^{-3}.

Acknowledgement

The authors wish to thank Mr K. Yoshida, Kyoto University, for his kind experimental supports.

References

[1] S.J. Zinkle, C. Kinoshita, J. Nucl. Mater. 251 (1997) 200.
[2] K. Moritani, I. Takagi, H. Moriyama, J. Nucl. Mater. 326 (2004) 106.
[3] K. Oda, T. Yoshio, J. Am. Ceram. Soc. 80 (1997) 3233.
[4] B.D. Evans, J. Nucl. Mater. 219 (1995) 202.
[5] A. Al Ghamdi, P.D. Townsend, Nucl. Instrum. and Methods B46 (1990) 133.
[6] A. Morono, E.R. Hodgson, J. Nucl. Mater. 249 (1997) 128.
[7] E.R. Hodgson, A. Delgado, J.L. Alvarez Rivas, Phys. Rev. B18 (1978) 2911.
[8] A. Morono, E.R. Hodgson, J. Nucl. Mater. 307–311 (2002) 1246.
[9] D.F. Mariani, J.L. Alvarez Rivas, J. Phys. C: Solid St. Phys. 11 (1978) 3499.
[10] K. Atobe, N. Nishimoto, M. Nakagawa, Phys. Status Solidi A 89 (1985) 155.
[11] R.L. Swank, F.C. Brown, Phys. Rev. 130 (1963) 34.